





# Folded Context Condensation in Path Integral Formalism for Infinite Context Transformers

Won-Gi Paeng<sup>\*</sup>, Daesuk Kwon<sup>\*</sup>, Kyungwon Jeong<sup>\*</sup>, and Honggyo Suh<sup>\*</sup>

<sup>\*</sup>Hyntel, Inc., Seoul 04783, Korea

Corresponding author: Won-Gi Paeng, wgpaeng@hyntel.net

**Abstract**—In this work, we present a generalized formulation of the Transformer algorithm by reinterpreting its core mechanisms within the framework of Path Integral formalism. In this perspective, the attention mechanism is recast as a process that integrates all possible transition paths leading to future token states, with temporal evolution governed by the Feed-Forward Network. By systematically mapping each component of the Transformer to its counterpart in the Path Integral formulation, we obtain a more compact and efficient representation, in which the contextual information of a sequence is condensed into memory-like segments. These segments are recurrently processed across Transformer layers, enabling more effective long-term information retention. We validate the effectiveness of this approach through the Passkey retrieval task and a summarization task, demonstrating that the proposed method preserves historical information while exhibiting memory usage that scales linearly with sequence length. This contrasts with the non-linear memory growth typically observed in standard attention mechanisms. We expect that this quantum-inspired generalization of the Transformer architecture will open new avenues for enhancing both the efficiency and expressiveness of future Transformer models.

## I. INTRODUCTION

Transformers architecture [1] has revolutionized natural language processing (NLP) by demonstrating unparalleled effectiveness in capturing long-range dependencies and enabling scalable, parallelized computation. Unlike earlier Recurrent Neural Network (RNN) based models, which process sequences sequentially and suffer from vanishing gradient issues [2], Transformers leverage self-attention mechanisms to establish global dependencies across tokens, leading to significant improvements in contextual reasoning and coherent text generation. This architectural advantage has propelled Transformers to the forefront of modern NLP, underpinning the development of large-scale language models (LLMs) with remarkable generative capabilities.

Despite their empirical success, the theoretical foundations of Transformer architectures remain incomplete. While extensive research has explored their scaling properties [3], emergent behaviors [4], and empirical performance [5], [6], these studies provide limited insight into the fundamental mechanisms governing Transformer architectures. In particular, there is a lack of rigorous theoretical formulations explaining how information propagates through layers and how hierarchical structures are captured within Transformer models. This gap in understanding limits the interpretability and optimization

of Transformer-based architectures and presents challenges in extending their capabilities systematically.

Another critical limitation of Transformers is their computational inefficiency when handling long sequences. The self-attention mechanism inherently scales quadratically with sequence length in both memory and computation, making it impractical to process extensive contexts within a single pass. This limitation hinders the retention of dependencies across long documents, dialogues, or continuous interactions, prompting the development of alternative strategies such as Infini-Attention [7], which restructures the self-attention mechanism by introducing a hybrid memory system that allows interaction between local context tokens and external memory components, leveraging a linear attention [8] framework to reduce computational overhead. Another innovative solution is Titans [9], which incorporates trainable neural long-term memory, enabling the model to retain and retrieve past contextual information beyond traditional Transformer constraints. However, these methods often introduce external memory components that do not engage with the Feed-Forward Network, which we believe may reduce their ability to convey context information across segments.

To address these challenges, we propose a novel theoretical generalization of the Transformer architecture based on the Path Integral formalism [10]—a fundamental framework in quantum mechanics used to describe the evolution of dynamical systems. The Path Integral approach models a system’s transition by summing over all possible trajectories, each weighted by an exponential factor of the action. Based on this principle, we reinterpret the attention mechanism in Transformers as integrating over all potential transition paths leading to future token states. This perspective allows us to establish a formal analogy between token state evolution in Transformers and the summation of quantum paths, with the transition dynamics governed by the Least-action principle.

Through this framework, we introduce a structured context delivery mechanism that enhances long-term dependency modeling while maintaining computational efficiency. By treating each Transformer layer as a time-evolution operator acting on token states, we derive a formulation in which contextual information is recurrently processed across layers. This approach effectively condenses past states into memory-like segments that evolve over time, thereby reducing memory complexity to scale linearly with sequence length while preserving expressive power. Unlike traditional self-attention, which explicitly

computes pairwise token interactions within a sequence at each step, our method naturally integrates historical context in the separated segments of a sequence without incurring quadratic computational costs.

Building on this theoretical foundation in Section II, we present an implementation in Section III that extends Transformer architectures with a time-evolving memory buffer. This structured approach ensures that past token representations contribute constructively to future states, akin to propagators in quantum field theory. Our proposed model enables efficient long-range dependency modeling while significantly reducing memory consumption compared to conventional Transformers.

In section IV, we validate our approach through empirical evaluations, including the Passkey retrieval and summarization tasks. Our experimental results demonstrate that the proposed method achieves performance on par with the base model in contextual recall, while delivering superior memory efficiency compared to the base Llama-3.2 models [13].

By unifying Transformer architectures with principles from quantum mechanics, this work provides a novel theoretical perspective that enhances both interpretability and efficiency. We anticipate that this Path Integral-based formulation will open new avenues for developing scalable and theoretically grounded AI models, enabling more robust processing of long-range dependencies in natural language and beyond.

## II. GENERALIZATION OF TRANSFORMER IN PATH INTEGRAL FRAMEWORK

The Path Integral approach provides a probabilistic framework for describing the evolution of a particle state by summing over all possible trajectories, with each path contributing according to a phase factor determined by the action. The foundation of this formulation lies in the Principle of Least Action, which states that the motion of a system follows a trajectory that minimizes (or extremizes) the action. In quantum mechanics, the Path Integral formulation extends the concept of the Least Action Principle by incorporating all possible paths leading to a future state, with their probability amplitudes interfering constructively or destructively.

Building upon this interpretation, we propose a novel generalization of the Transformer mechanism using the Path Integral formalism. In standard Transformers, the attention operation first determines the relationships between tokens within a sequence, followed by the Feed-Forward Network processing this contextualized information. This process bears a strong resemblance to the way quantum states evolve over time through the summation over all possible paths. By drawing on this analogy in the left side of Fig. 1, we reinterpret the transformation of a token vector through Transformer layers as the time evolution of a token state, where each token traverses multiple interaction pathways before contributing to the final output. Specifically, when we consider a case that a token state  $|x_i, t_n\rangle$  at position  $x_i$  in a sequence and time  $t_n$  temporally evolves to the state  $|x_i, t_{n+1}\rangle$  at position  $x_i$  and time  $t_{n+1}$ , we

can formulate this transition within a Path Integral framework as follows:

$$|x_i, t_{n+1}\rangle = \mathcal{N} \sum_{\text{all paths}} \mathcal{T} \exp\left(\frac{i}{\hbar} \int_{t_n}^{t_{n+1}} \mathcal{L} dt\right) |x_i, t_n\rangle \quad (1)$$

where  $\mathcal{L}$  is the Lagrangian of the Least Action Principle,  $\mathcal{N}$  is overall normalization factor to the contribution of all possible paths and  $\mathcal{T}$  is the operator of the time-ordered product. In the condition  $\Delta t = \frac{t_{n+1}-t_n}{N} \rightarrow 0$ , the equation (1) can be rewritten as

$$|x_i, t_{n+1}\rangle = \mathcal{N} \sum_{\text{all paths}} \mathcal{T} \left\{ \prod_{j=1}^N \exp\left(\frac{i}{\hbar} \mathcal{L}(t_n + j\Delta t) \Delta t\right) \right\} |x_i, t_n\rangle. \quad (2)$$

To consider the all possible paths in the way from  $t_n$  to  $t_{n+1}$ , we input the identity matrix as

$$I_j = \mathcal{N}_j \sum_k |x_k, t_{n,j}\rangle \langle x_k, t_{n,j}| \quad (3)$$

with the normalization factor  $\mathcal{N}_j$  at each time  $t_{n,j} \equiv t_n + (j-1)\Delta t$ , which supposes transitions to the all possible token states at  $t_{n,j}$ . Here, we note that  $x_k$  means  $k$ -th token position which is different from the ordinary position in space-time. Then, finally we get

$$|x_i, t_{n+1}\rangle = \mathcal{N} \mathcal{T} \left\{ \prod_{j=1}^N \left[ \exp\left(\frac{i}{\hbar} \mathcal{L}(t_n + j\Delta t) \Delta t\right) \mathcal{N}_j \sum_k |x_k, t_{n,j}\rangle \langle x_k, t_{n,j}| \right] \right\} |x_i, t_n\rangle. \quad (4)$$

In particular, we take into account the time evolution of the state from  $t_n + (j-1)\Delta t$  to  $t_n + j\Delta t$ , from the equation (4) as

$$|x_i, t_n + j\Delta t\rangle = \exp\left(\frac{i}{\hbar} \mathcal{L}(t_n + j\Delta t) \Delta t\right) \mathcal{N}_j \sum_k |x_k, t_{n,j}\rangle \langle x_k, t_{n,j} | x_i, t_n \rangle \quad (5)$$

which is illustrated in the right side of Fig. 1.

From (5), we induce the attention and neural net structure of the  $j$ -th Transformer layer as

$$X'_i = \text{softmax} \left[ \frac{X_i W_Q W_K^T}{\sqrt{d_E}} [\dots \ X_{k-1}^T \ X_k^T \ \dots] \right] \begin{pmatrix} \dots \\ X_{k-1} \\ X_k \\ \dots \end{pmatrix} W_V W_{FF}. \quad (6)$$

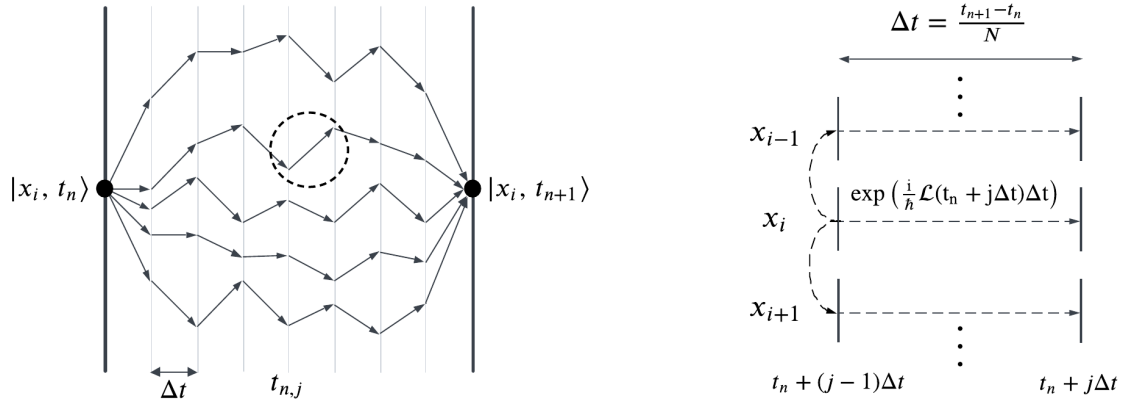


**Fig. 1:** Visualization of token state evolution in the Path Integral framework. The state  $|x_i, t_n\rangle$  at time  $t_n$  evolves through multiple interaction pathways before reaching  $|x_i, t_{n+1}\rangle$  (left side). Each evolution from  $t_{n,j}$  to  $t_{n,j} + \Delta t$  can be described as the transitions to all possible token states and the temporal evolutions of the projection states (right side).

for the position and token embedded state on the position  $i$ ,  $X_i \in \mathbb{R}^{d_E}$ , transforming to the context vector  $X'_i$  of the Transformer by the following correspondence,

$$|x_i, t_{n,j}\rangle \Leftrightarrow Q^T = W_Q^T X_i^T \quad (7)$$

$$\langle x_k, t_{n,j} | \Leftrightarrow K = X_k W_K \quad (8)$$

$$|x_k, t_{n,j}\rangle \Leftrightarrow V^T = W_V^T X_k^T \quad (9)$$

$$\exp\left(\frac{i}{\hbar} \mathcal{L}(t_n + j\Delta t) \Delta t\right) \Leftrightarrow W_{FF}^T \quad (10)$$

$$|x_i, t_n + j\Delta t\rangle \Leftrightarrow X_i'^T, \quad (11)$$

where  $FF$  stands for Feed-Forward Network and  $W_Q, K, V \in \mathbb{R}^{d_E \times d_M}$  are query, key and value matrices of the Transformer. Here we ignored multi-head attention for simplicity.

We introduced the concept of time into the Transformer structure by generalizing Transformers in the Path Integral framework and finding correspondences between them. The Transformer can be reinterpreted as the temporal evolution of an input token, and attention can be understood as a transition of an input token state to all possible token states in the same timeline. As the input token passes through each layer of Transformers, the time evolution is achieved, which can be interpreted as traversing all possible positional and temporal paths. Then, by reducing the cross entropy loss between targets and the output of Transformers, Transformers are trained to find the Least Action path of the Path Integral, which can be captured by the following equation as

$$-\ln |\mathcal{M}_{ij}|^2 = -\ln \left| \langle i | \mathcal{N} \sum_{\text{all paths}} \mathcal{T} \exp\left(\frac{i}{\hbar} \int \mathcal{L} dt\right) | j \rangle \right|^2, \quad (12)$$

which cross-entropy loss of the Transformers is calculated by the transition amplitude between two states through path-integral. As the model is trained, the cross-entropy loss becomes decreasing. Then, to get larger prediction probability as smaller cross-entropy loss, the paths with high frequency are canceled out so that the only paths carrying low valued-actions survive, which achieves the Least Action Principle.

This may explain why attention-based Transformers perform so well when estimating the next token state. In the next section, we will introduce an application from the perspective of time evolution.

### III. FOLDED CONTEXT CONDENSATION: THE IMPLEMENTATION OF THE MODEL

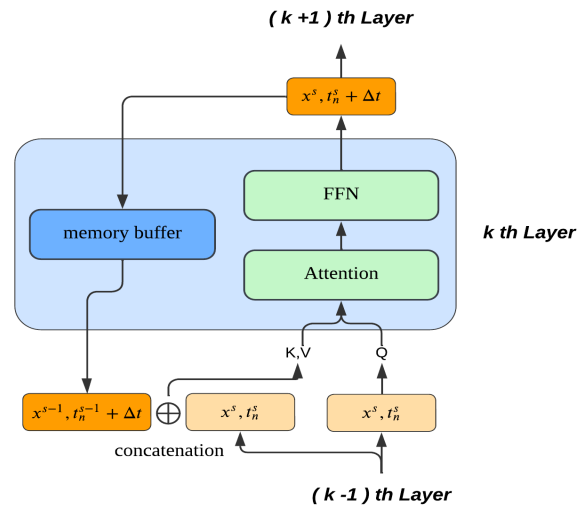


**Fig. 2:** Underlying architecture of the model. A segment  $|x^s, t_n^s\rangle$  from the previous layer is projected into a query and also concatenated with time-evolved memory buffer  $|x^{s-1}, t_n^{s-1} + \Delta t\rangle$  to be key and value. The output of the current layer will be saved as a memory buffer and retrieved when the next segment arrives.

We consider a certain case of combining outputs of Transformer layers for separated input segments. A length  $L$  sequence is divided into segments of length  $l$ , such that  $N_s = L/l$ , and then the tokens in each segment are put into the Transformer layers sequentially. Here, we suggest how to deliver the information of a segment to another segment in the Transformer architecture. In the previous section, by reinterpreting the Transformers in the Path Integral framework, we find that the Feed-Forward Network makes the temporal

evolution of the token state. Therefore, it is expected that there can be a phase difference between the token states in separated segments.

As shown in Fig. 2, we define a token state  $|x_i^s, t_n^s\rangle$  on the position  $i$  in  $s$ -th segment and the token state evolves in a Transformer layer as

$$|x_i^s, t_n^s + \Delta t\rangle = \exp\left(\frac{i}{\hbar}\mathcal{L}(t_n^s + \Delta t) \Delta t\right) \mathcal{N} \sum_k |x_k^s, t_n^s\rangle \langle x_k^s, t_n^s | x_i^s, t_n^s\rangle \quad (13)$$

with  $i = 1, \dots, l$  and  $s = 1, \dots, N_s$ . The temporal evolution of the token state makes the phase shift of the token state, and each layer gives a different phase shift. If the phase difference between different segments is not properly handled, tokens from separated segments may interfere destructively, leading to the loss of important historical information from previous segments. Here is a solution to make the constructive interference between the segments, that is we impose a time gap between the segments to be periodical, which can be accomplished by applying recurrent Transformer layer with the segments. For example, we input  $s - 1$ -th and  $s$ -th segments in parallel into a Transformer layer as

$$|x_i^s, t_n^s + \Delta t\rangle = \exp\left(\frac{i}{\hbar}\mathcal{L}(t_n^s + \Delta t) \Delta t\right) \mathcal{N} \sum_k (|x_k^{s-1}, t_n^{s-1} + \Delta t\rangle \langle x_k^{s-1}, t_n^{s-1} + \Delta t| + |x_k^s, t_n^s\rangle \langle x_k^s, t_n^s|) |x_i^s, t_n^s\rangle, \quad (14)$$

where we apply the boundary condition as

$$t_n^s = t_n^{s-1} + \Delta t \quad (15)$$

by concatenating the output of the layer for  $x^{s-1}$  with the input of the layer for  $x^s$  step in Fig. 2. In this way, every segment will line up with an integer-multiple time gap so that every segment contributes to constructive interference.

This periodic temporal evolution and the transition between  $s - 1$ -th and  $s$ -th segments can be presented as

$$X^{s'} = \text{softmax}\left(\frac{Q^s}{\sqrt{d_E}} [K^{s-1T} \quad K^{sT}]\right) \begin{pmatrix} V^{s-1} \\ V^s \end{pmatrix} W_{\text{FF}} \quad (16)$$

in a Transformer layer shown as Fig. 2, where  $Y^s = X^s W_Y$  with  $X^s \in \mathbb{R}^{l \times d_E}$  and  $Y = Q, K, V$ . The masking for the attention matrix is given in Fig. 3. We note that the all dot-product attention between  $Q^s$  and  $K^{s-1}$  are not masked to relate all contextual information from past segments to the current query. Then, every layer has a recurrent structure transferring the information from  $s - 1$ -th to  $s$ -th segments.

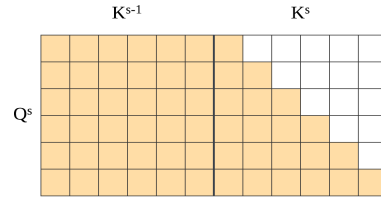


**Fig. 3:** The attention mask is divided into two regions:  $K^{s-1}$  represents memory keys that allow full attention across all positions, while  $K^s$  represents current keys, where attention is restricted with a causal masking pattern.  $Q^s$  denotes the current query, interacting selectively with both  $K^{s-1}$  and  $K^s$ .

We explain how we can implement the model to reduce resources and apply it to multi-layer Transformers. When training Transformers, the attention mechanism is one of the most resource-consuming components, scaling quadratically with the input length. So, we focus on how we reduce the token length for attention while preserving the quality of the prediction by conserving the historical information through the sequence divided by the segments. We suppose that the token sequence is divided by  $N_s(L/l)$  segments having the same token length  $l$  as in the previous section, and the segments are sequentially put into the multi-layer Transformers as shown in Fig. 4. First, token embedding is performed for each segment, where each has a different position ids. Then, the  $s$ -th segment is concatenated with the previous recurrent  $s - 1$ -th segment to be put into the attention as length  $2l$  key and value vectors while the query has length  $l$  as in Fig. 2. After the output of the attention is added up with the residual unit, it is put into the Feed-Forward Network. Finally, the outputs of the multi-layer Transformers are matched with each target for each corresponding segment to get the cross-entropy loss which is summed up as

$$L_{\text{total}} = \sum_{s=1}^{N_s} L_s, \quad (17)$$

where  $L_s$  is a cross-entropy loss for  $s$ -th segment. The model is trained to reduce the total cross-entropy loss,  $L_{\text{total}}$ .

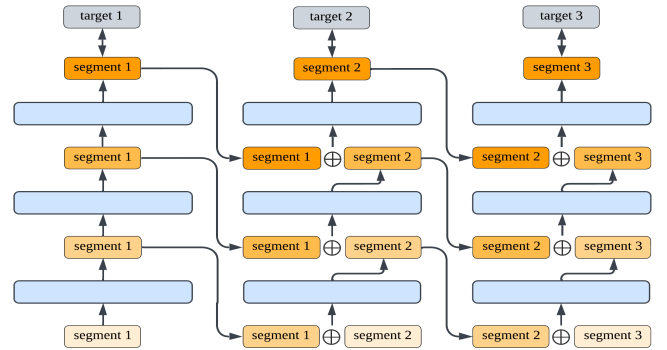


**Fig. 4:** Each output of each layer for input segment is preserved as a memory buffer. Then, the memory buffer is concatenated with the current segment and takes part in the attention.

## IV. EXPERIMENTS

In this section, we evaluate the effectiveness and efficiency of the proposed Folded Context Condensation mechanism (hereafter referred to as the **Condensation model**) in comparison to the Llama-3.2 model (hereafter referred to as the Llama model). First, we demonstrate that the Condensation model achieves significantly lower memory consumption than the Llama model under comparable conditions, and we further evaluate its training speed across varying sequence lengths to assess whether the Condensation mechanism offers practical computational advantages. Next, we validate the Condensation model’s ability to propagate information across distant segments using a passkey retrieval task, which tests whether critical information from earlier segments can be effectively retrieved after processing subsequent segments. Finally, we evaluate the ability to perform long-document summarization using the Booksum dataset, showing that the model is capable of processing extended contexts and generating coherent summaries without quality degradation, even as the input length increases. At the end of this section, we will demonstrate through attention score visualization that, with Folded Context Condensation, the contextual information from preceding segments is not lost and continues to participate in the attention process together with the currently processed segment.

### A. Memory usage measurement & Speed Comparison

Compared to the original Transformer model, the Condensation model splits a sequence of length  $L$  into  $N_s$  fixed-length segments. This segmentation reduces the memory complexity of the attention computation from  $\mathcal{O}(L^2)$  to  $\mathcal{O}(N_s l^2)$ , where  $l$  denotes the segment length. By fixing the segment length, the overall memory requirement transitions from quadratic to linear growth with respect to the total sequence length. The effectiveness of this approach was validated through direct comparison with the Llama model.

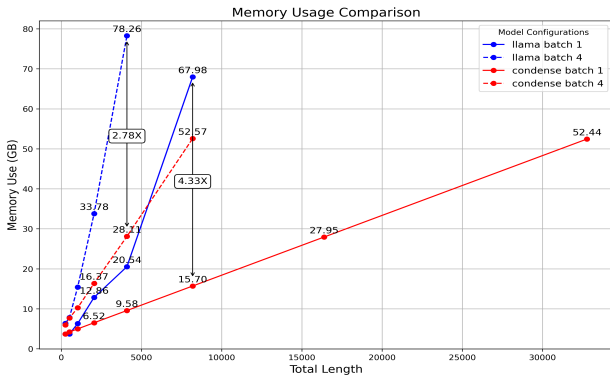


Fig. 5: Memory usage comparison as a function of total sequence length. The plot illustrates memory consumption (in GB) for Condensation and Llama models across batch sizes 1 and 4.

The Condensation model, represented by red lines in Figure 5, exhibits a linear increase in memory usage proportional to the sequence length. In contrast, the Llama model, shown with blue lines, deviates from this linear trend,

indicating a more complex memory scaling behavior. At a total sequence length of 8K, the Llama model consumed 4.33 times more memory compared to our Condensation model with batch 1. Similarly, at 4K, the Llama model required 2.78 times more memory than the Condensation model with batch 4.

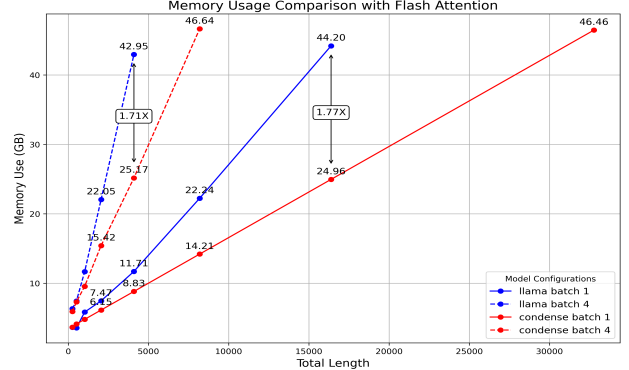


Fig. 6: Memory usage comparison by sequence length with FlashAttention.

Fig. 6 presents a comparison of memory usage as a function of total sequence length with FlashAttention [11] enabled. At a sequence length of 16K, the Llama model consumed approximately 1.77 times more memory than the Condensation model with a batch size of 1. Similarly, at a sequence length of 4K, the Llama model required approximately 1.71 times more memory than the Condensation model when using a batch size of 4.

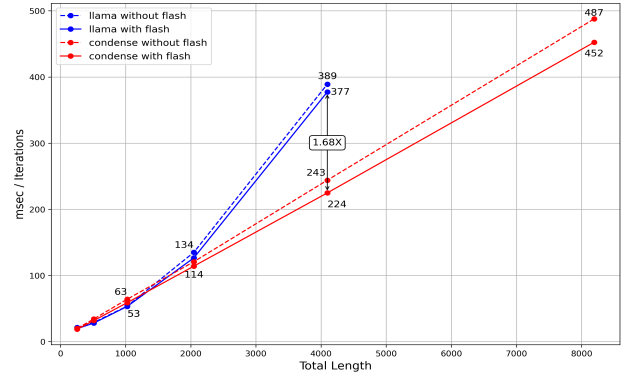


Fig. 7: Training Speed Comparison by Sequence Length with and without FlashAttention

Fig. 7 presents a comparison of training speeds between the Condensation and Llama models across varying sequence lengths, evaluated both with and without FlashAttention. For shorter sequences (under 2K tokens), the Llama model achieves faster training speeds than the Condensation model, regardless of whether FlashAttention is applied. However, as sequence length increases beyond 2K tokens, the Condensation model outperforms Llama in terms of speed, particularly for sequences of 4K and 8K tokens, where Condensation achieves lower iteration times. At a sequence length of 4K, Condensation with FlashAttention processes training iterations approxi-

mately 1.68 times faster than Llama with FlashAttention. Also, the results demonstrate that the effect of FlashAttention is relatively minor for both models across all sequence lengths, with only marginal improvements observed in training speed.

Configuration	Condensation	Llama
Original model	Llama-3.2-1B	Llama-3.2-1B
Number of Layers	4	4
Hidden size	512	512
Segment Length	256	-
Trainable Parameters	126M	126M
Head Dimension	64	64
Number of Heads	32	32
Number of Key/Value Heads	8	8
Number of GPUs	1	1
GPU	H100	H100

TABLE I: Configuration for memory & speed experiment

The memory and speed experiments were conducted using the configurations shown in Table I, with both the Condensation and Llama models tested on a single NVIDIA H100 GPU. All memory experiments for the Condensation model were conducted using a segment length of 256. To compare the impact of the Condensation mechanism on memory usage and training speed, we used a reduced-scale model with 126 million trainable parameters.

The results indicate that, in terms of memory efficiency, the Condensation architecture effectively reduces memory usage by flattening the memory growth curve, enabling the processing of significantly longer sequences with reduced memory overhead. In terms of training speed, however, the Condensation model exhibits slower iteration times for shorter sequences compared to Llama. As the sequence length increases beyond 2K tokens, the Condensation model becomes more efficient in terms of speed, demonstrating faster iteration times than Llama at 4K and 8K tokens. In the current implementation, the Condensation model processes input sequences sequentially at the granularity of each segment, which limits the potential for significant speed improvements. However, future enhancements incorporating pipeline-style parallelism could further improve Condensation’s processing efficiency, particularly for long sequences.

### B. Passkey retrieval task

The Passkey retrieval task embeds a passkey (a four-digit number) within a long document containing unrelated text and challenges the model to retrieve it. This task serves as a simple yet intuitive benchmark for evaluating whether the model retains critical information from previous segments or disregards it in favor of new input. In this study, we used the Llama-3.2-1B model as a baseline with Condensation logic applied, and the model was continuously pretrained on the Fine-web dataset [12] to adapt to the new logic with 512 segment length. The model was then finetuned on the Passkey task dataset starting with a sequence length of 2K, followed by incremental increases to 4K, 8K, and ultimately 16K, which was more efficient than directly finetuning to 16k. The model

was finetuned up to 16k because of the constraints of memory resources. We evaluated the Condensation model further on 32K and 64K length datasets.

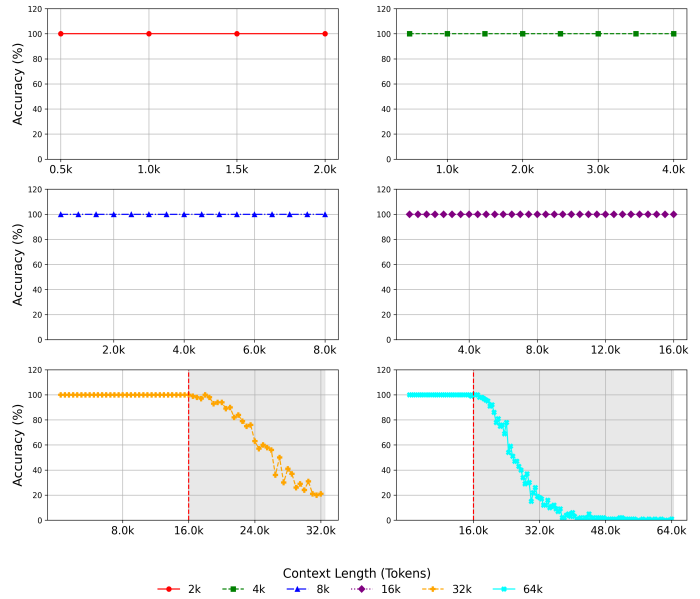


Fig. 8: Passkey retrieval accuracy across different total sequence lengths. Each subplot represents evaluation at a specific context length, ranging from 2K to 64K tokens. The vertical dashed red line indicates the sequence length at which the model was fine-tuned. Accuracy remains consistently high within the fine-tuned length, while performance degrades when evaluated on significantly longer sequences, highlighting the challenge of zero-shot generalization to unseen context lengths.

The Fig. 8 depicts evaluation results for sequence lengths of 2K, 4K, 8K, 16K, and zero-shot evaluations at 32K and 64K. (Note that each results were evaluated with a 16K length finetuned model) The y-axis represents accuracy, while the x-axis indicates the depth, defined as the absolute position where the passkey is embedded. The model demonstrated the ability to effectively convey information across segments, achieving 100% accuracy within the sequence lengths on which it was fine-tuned. However, performance declined when evaluated on sequences longer than the model’s fine-tuning range. Enabling the model to retrieve passkeys beyond the finetuning range in a zero-shot manner is a potential avenue for future work.

### C. Summarization task

While the passkey task is designed to evaluate the model’s ability to transfer information across segments, the summarization task assesses its capability to comprehend and integrate the full context. For this purpose, we scaled the model to Llama-3.2-3B and conducted continual pretraining on the Fine-web dataset [12] with 512 segment length. Subsequently, the model was first finetuned on the CNN/DailyMail dataset [16], which comprises a collection of news articles and their corresponding highlights. The highlights were treated as summaries, while the news articles served as the contextual input. To train the model on longer contexts, the Booksum dataset was filtered to include sequences of 5.5K length and combined with CNN/DailyMail for the second experiment.

Two baseline models were prepared for benchmarking: Llama-3.2-3B-Instruct and Llama-3.2-3B fine-tuned exclusively on the CNN/DailyMail dataset. We employed a simple generation setting with a temperature of 0.3, generating 256 tokens without beam search.

Model (finetuned length)	Input Length	ROUGE-1/2/L (F1)
Condensation (3K)	0-512	0.4501 / 0.2232 / 0.3242
	512-1024	0.4368 / 0.2008 / 0.3022
	1024+	0.3996 / 0.1510 / 0.2566
	Overall	<b>0.4292</b> / 0.1917 / <b>0.2942</b>
Condensation (5.5K)	0-512	0.4532 / 0.2260 / 0.3258
	512-1024	0.4337 / 0.2002 / 0.3007
	1024+	0.3985 / 0.1501 / 0.2557
	Overall	0.4282 / <b>0.1918</b> / 0.2936
Full-Finetuned (3K)	0-512	0.4432 / 0.2155 / 0.3162
	512-1024	0.4271 / 0.1953 / 0.2947
	1024+	0.3999 / 0.1650 / 0.2627
	Overall	0.4231 / 0.1913 / 0.2905
Instruction model	0-512	0.3354 / 0.1376 / 0.2171
	512-1024	0.3191 / 0.1251 / 0.1985
	1024+	0.3022 / 0.1095 / 0.1820
	Overall	0.3180 / 0.1236 / 0.1981

**TABLE II:** Rouge (Recall-Oriented Understudy for Gisting Evaluation) scores [15] by model and input length. The Condensation model was further finetuned on 5.5K to see if there was any performance improvement with a longer context. Rouge scores for each range were recorded separately to see if performance decreases with longer inputs.

Remarkably, our model achieved higher Rouge scores (Rouge-1, Rouge-2, Rouge-L) on the CNN/DailyMail than the Llama-3.2-3B-Instruct model and comparable results to the Llama-3.2-3B model fine-tuned on the dataset in the table II. This demonstrates the model’s ability to effectively condense information from each segment into limited-sized context vectors.

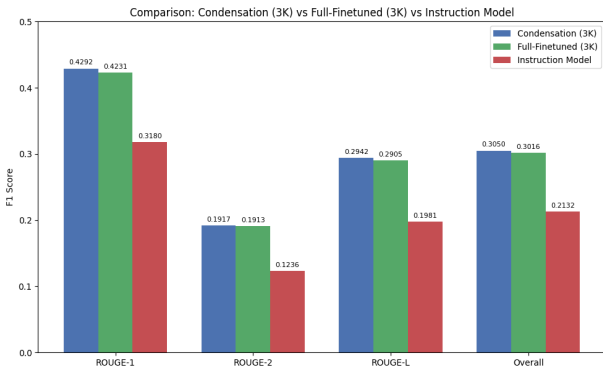


**Fig. 9:** ROUGE score comparison between three models: (1) Condensation 3B model fine-tuned on CNN/DailyMail with a 3K context length, (2) LLaMA-3.2-3B model fine-tuned on CNN/DailyMail with a 3K context length, and (3) LLaMA-3.2-3B Instruct model.

In Fig. 9, the Condensation model consistently outperforms the instruction-tuned model across all ROUGE metrics (ROUGE-1, ROUGE-2, and ROUGE-L) and achieves comparable performance to the fully fine-tuned Llama model, demonstrating its ability to effectively summarize long documents despite the segmented processing mechanism.

Fig. 10 visualizes attention scores in a Condensation model, showing attention matrices between segments 2-3, 4-5, and 6-7 across

Layers 1, 8, and 16. The input is the text in summary format with 4K total and 0.5K segment length, and we retrieved the attention score before applying softmax computation and rescaled with the Minmax scaling for visibility. Here we used an attention mask from Fig. 3. The matrices, with x- and y-axes ranging from 0 to 1K and 0 to 0.5K tokens respectively, use a color gradient (purple to yellow, 0.0 to 1.0) to represent attention weights. The visualization reveals that attention scores are well distributed across both  $K^{s-1}$  and  $K^s$ , indicating that the model effectively utilizes not only the current key but also the past key when processing hidden states. The early layer (Layer 1) tends to attend previous context as much as the current segment, the middle layer (Layer 8) and later layer (Layer 16) show diffused attention capturing broader relationships, suggesting a shift from the previous to current segment context understanding as the model progresses through blocks, with slight variations in intensity across blocks.

## V. CONCLUSION

Our work introduces a quantum-inspired reformulation of Transformer architectures by leveraging Path Integral formalism to reinterpret the attention mechanism as a dynamic, temporal evolution of token states. By incorporating temporal dynamics into token state representations, the proposed Path Integral formulation provides a theoretical foundation for understanding transformer layers and attention mechanisms. This framework connects theoretical insights with practical architectural design, allowing constructive interference between tokens to participate in attention across segments. It also suggests that relatively compact token representations can effectively condense contextual information in a recurrent manner. Our experimental evaluations—including passkey retrieval and summarization tasks—demonstrate that this approach achieves both superior memory efficiency and competitive performance across extended sequence lengths. This perspective offers a promising direction for designing novel Transformer architectures and exploring quantum-inspired algorithms, opening up opportunities for future research. We plan to further expand on these ideas and share subsequent findings in future publications. We hope this work serves as a foundation for a deeper theoretical understanding of Transformer architectures and contributes to bridging concepts from quantum mechanics and artificial intelligence.

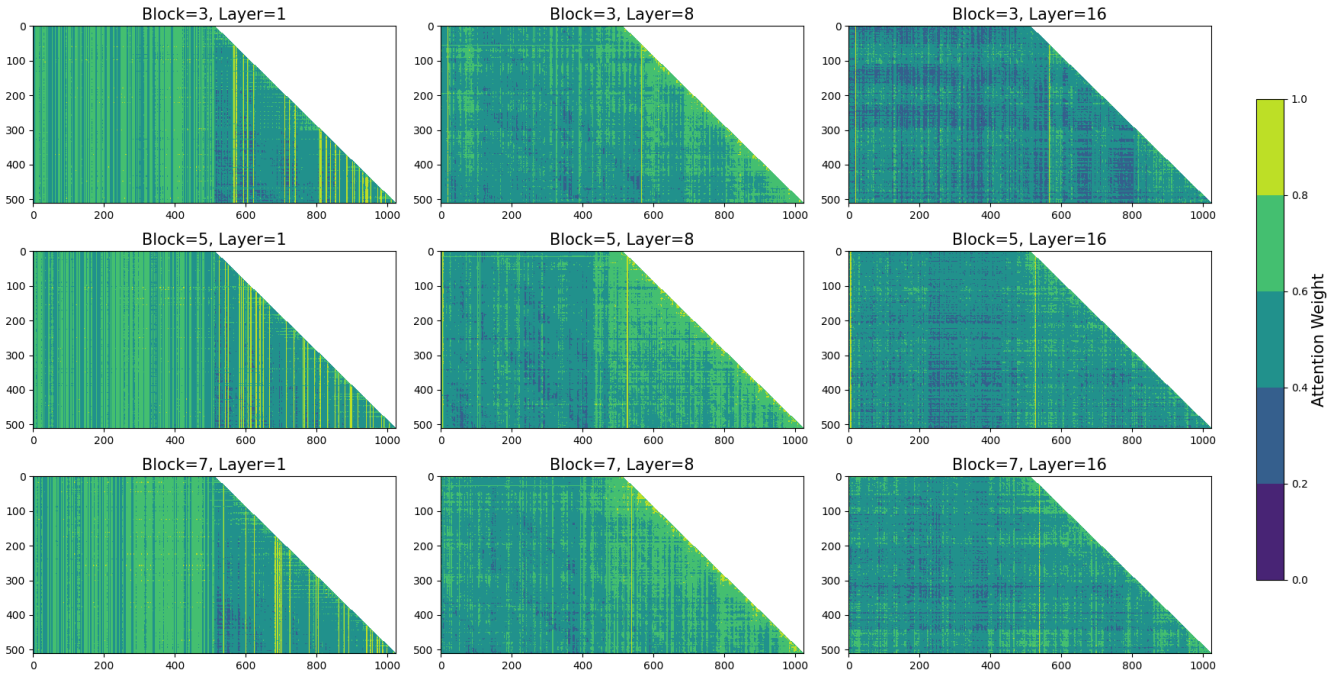


Fig. 10: Attention score of the Condensation model across different blocks and layers

Task Configuration	Passkey		Summarization			
	Pretrain	Finetuning	Pretrain	Finetuning	Finetuning	Finetuning
Model	Condensation	Condensation	Condensation	Condensation	Condensation	Llama
Original Model	Llama-3.2-1B	Llama-3.2-1B	Llama-3.2-3B	Llama-3.2-3B	Llama-3.2-3B	Llama-3.2-3B
Layer	16	16	28	28	28	28
Embedding Size	2048	2048	3076	3076	3076	3076
Trainable Parameters	1.2B	1.2B	3.2B	3.2B	3.2B	3.2B
Segment Length	512	512	512	512	512	512
Total Length	4K	2k/4k/8k/16k	5K	3K	5.5K	3K
Learning Rate	$6 \times 10^{-5}$ to $2 \times 10^{-5}$	$6 \times 10^{-5}$	$6 \times 10^{-5}$ to $6 \times 10^{-6}$	$6 \times 10^{-6}$ to $6 \times 10^{-7}$	$6 \times 10^{-6}$ to $6 \times 10^{-7}$	$6 \times 10^{-6}$ to $6 \times 10^{-7}$
Dataset	Fineweb-edu (filtered over 4K)	Passkey dataset	Fineweb-edu (filtered over 6K)	CNN/DailyMail	CNN/DailyMail + filtered Booksum	CNN/DailyMail
Training Steps	6491	500/300/1000/1000	9426	3700	3855	112
Validation Loss	2.323	$\simeq 0$	2.160	1.330	1.350	1.290

TABLE III: Configuration for passkey and Condensation experiments across pretraining and finetuning

## APPENDIX A PASSKEY RETRIEVAL AND SUMMARIZATION TASK CONFIGURATION

The table III presents the experimental configurations for pretraining and finetuning models on Passkey and Booksum tasks. For the Passkey task, a Condensation model based on Llama-3.2-1B with 16 layers and a 2048 embedding size was continuously pretrained on the Fineweb-edu dataset (filtered for sequences over 4K) and finetuned on the Passkey dataset, achieving a validation loss of 2.323 after continuous pretraining. For the Booksum task, a larger Condensation model based on Llama-3.2-3B with 28 layers and a 3076 embedding size was continuously pretrained on Fineweb-edu (filtered over 6K) and finetuned across two setups: (1) CNN/DailyMail, (2) CNN/DailyMail with filtered Booksum data. All experiments utilized the ZeRO-2 optimization [14], cosine learning rate decay, Bfloat16 mixed precision, and a global batch size of 64. We trained all models until we observed convergence of validation loss.

## APPENDIX B SUMMARIZATION TASK RESULTS

Fig. 11 compares the performance of the Condensation 3B model fine-tuned on a 5.5K context length against the LLaMA-3.2-3B Instruction model. Due to memory constraints, we could not train an LLaMA model with a 5.5K context length for direct comparison. The results show that the Condensation model consistently outperforms the instruction-tuned baseline across all ROUGE metrics (ROUGE-1, ROUGE-2, ROUGE-L), demonstrating the effectiveness of the Condensation mechanism in handling long-document summarization tasks, even at extended context lengths.

Fig. 12 presents a comparison between two Condensation 3B models: one fine-tuned on CNN/DailyMail combined with filtered BookSum data using a 3K context length, and the other fine-tuned on the same dataset with additional data using a 5.5K context length. The results indicate that extending the context length to 5.5K during training does not lead to significant performance degradation when



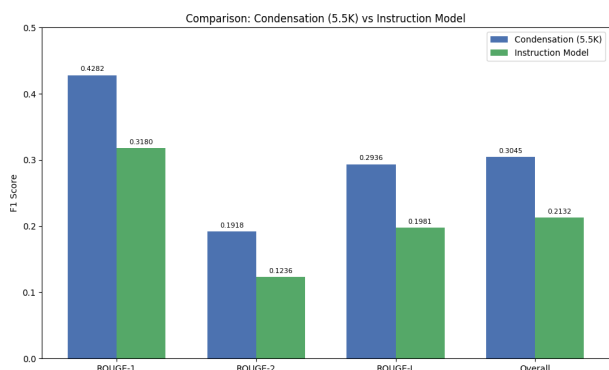


Fig. 11: Comparison of ROUGE scores between two models: (1) Condensation 3B model fine-tuned on CNN/DailyMail combined with filtered BookSum data using a 5.5K context length, and (2) LLaMA-3.2-3B Instruct model.

evaluated on the CNN/DailyMail dataset.

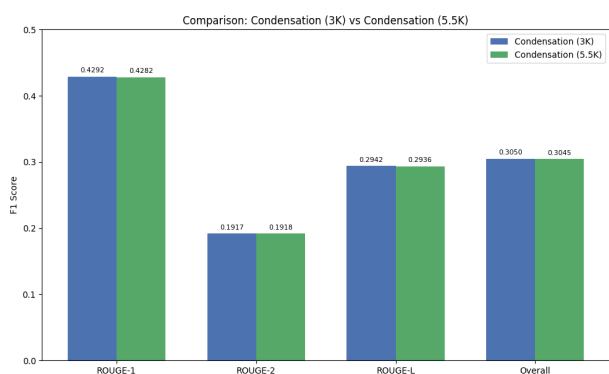


Fig. 12: Comparison of ROUGE scores between two Condensation 3B models: (1) Condensation 3B fine-tuned on CNN/DailyMail combined with filtered BookSum data using a 3K context length, and (2) Condensation 3B fine-tuned on the same dataset with additional data using a 5.5K context length.

## APPENDIX C PASSKEY RETRIEVAL TASK

The following example illustrates the input format used in the Passkey retrieval task. The goal of this task is to identify and memorize a specific four-digit passkey embedded within a large amount of irrelevant text. The model must extract and recall this passkey when prompted.

---

### Input :

There is a critical piece of information hidden within a large amount of irrelevant text. Your task is to locate it and remember it carefully. I will test your ability to recall this information.

The grass is green. The sky is blue. The sun is yellow. Here we go. There and back again. (repeat  $x$  times)

**The passkey is 9054. Remember it carefully. 9054 is the passkey.**

The grass is green. The sky is blue. The sun is yellow. Here we go. There and back again. (repeat  $y$  times)

What is the passkey? The passkey is

---

**Expected Output:** 9054

## APPENDIX D SUMMARIZATION TASK

The following example illustrates the input format used in the Summarization task. The goal of this task is to read a lengthy piece of text and provide a concise summary of its main points when prompted.

---

### Input :

Summarize this text :

### article

----

Summary :

---

**Expected Output:** Summary of this article

## REFERENCES

- [1] A. Vaswani et al., "Attention is all you need," presented at the NIPS., Long Beach, CA, USA, Dec. 4-9, 2017.
- [2] Y. Bengio, P. Simard, and P. Frasconi, "Learning long-term dependencies with gradient descent is difficult," *IEEE Trans. Neural Netw.*, vol. 5, no. 2, pp. 157-166, Mar. 1994.
- [3] J. Kaplan et al., "Scaling Laws for Neural Language Models," 2020, *arXiv:2001.08361*.
- [4] J. Wei et al., "Emergent Abilities of Large Language Models," 2022, *arXiv:2206.07682*.
- [5] A. Srivastava et al., "Beyond the Imitation Game: Quantifying and extrapolating the capabilities of language models," 2022, *arXiv:2206.04615*.
- [6] D. Hendrycks et al., "Measuring Massive Multitask Language Understanding," 2020, *arXiv:2009.03300*.
- [7] T. Munkhdalai, M. Faruqi, and S. Gopal, "Leave No Context Behind: Efficient Infinite Context Transformers with Infini-attention," 2024, *arXiv:2404.07143*.
- [8] Z. Shen et al., "Efficient Attention: Attention with Linear Complexities," 2018, *arXiv:1812.01243*.
- [9] B. Ali, Z. Peilin, and M. Vahab, "Titans: Learning to Memorize at Test Time," 2024, *arXiv:2501.00663*.
- [10] R. P. Feynman and A. R. Hibbs, "Quantum Mechanics and Path Integrals," New York, NY, USA: McGraw-Hill, 1965.
- [11] T. Dao, "FlashAttention-2: Faster Attention with Better Parallelism and Work Partitioning," 2023, *arXiv:2307.08691*.
- [12] Guilherme et al., "The FineWeb Datasets: Decanting the Web for the Finest Text Data at Scale," 2024, *arXiv:2406.17557*.
- [13] G. Aaron et al., "The Llama 3 Herd of Models," 2024, *arXiv:2407.21783*.
- [14] R. Samyam et al., "ZeRO: Memory Optimizations Toward Training Trillion Parameter Models", 2019, *arxiv:1910.02054*.
- [15] C. Lin, "ROUGE: A Package for Automatic Evaluation of Summaries.", *Text Summarization Branches Out, Post-Conference Workshop of ACL*, Barcelona, Spain, 2004, pp. 74-81.
- [16] M. H. Karl et al., 2015, "abisee/cnn\_dailymail", Huggingface. [Online]. Available: [https://huggingface.co/datasets/abisee/cnn\\_dailymail](https://huggingface.co/datasets/abisee/cnn_dailymail)